Chemical Engineering Journal 319 (2017) 48–56

Contents lists available at ScienceDirect

Chemical Engineering Journal

journal homepage: www.elsevier.com/locate/cej

Selective liquid-phase hydrogenation of fructose to D-mannitol over copper-supported metallic nanoparticles

J. Zelin [a], C.I. Meyer [a], S.A. Regenhardt [a], V. Sebastian [b,c], T.F. Garetto [a], A.J. Marchi [a,*]

[a] Catalysis Science and Engineering Research Group (GICIC), INCAPE, UNL-CONICET, Colectora Ruta Nac. N° 168 Km 0, 3000 Santa Fe, Argentina
[b] Department of Chemical Engineering, Aragon Institute of Nanoscience (INA), University of Zaragoza, Campus Río Ebro-Edificio I+D, C/ Poeta Mariano Esquillor S/N, 50018 Zaragoza, Spain
[c] CIBER de Bioingeniería, Biomateriales y Nanomedicina (CIBER-BBN), C/Monforte de Lemos 3-5, Pabellón 11, 28029 Madrid, Spain

HIGHLIGHTS

- Metal Cu nanoparticles on SiO_2 were attained by precipitation-deposition method at pH ≅ 7.
- An 80% yield in D-mannitol was achieved over a Cu/SiO_2 catalyst without using co-catalysts.
- Strong fructose adsorption on large metal Cu particles reduces activity and D-mannitol yield.
- Interaction of metallic Cu nanoparticles with acid/basic sites favors isomerization to glucose.

GRAPHICAL ABSTRACT

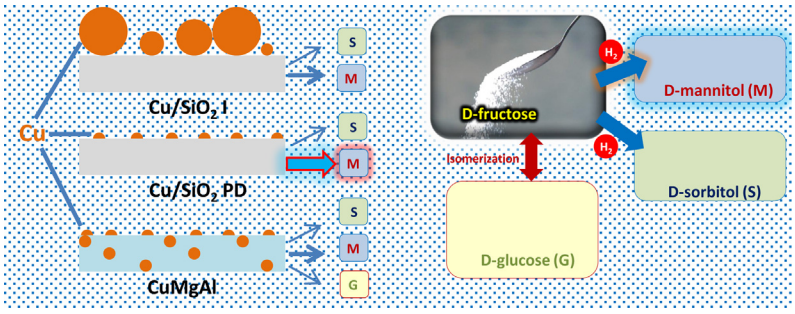

ARTICLE INFO

Article history:
Received 1 November 2016
Received in revised form 22 February 2017
Accepted 23 February 2017
Available online 27 February 2017

Keywords:
D-Fructose
D-mannitol
Liquid-phase hydrogenation
Cu-based catalyst

ABSTRACT

The selective liquid-phase hydrogenation of D-fructose was studied on Cu-based catalyst, using an ethanol-water (70:30) mixture as solvent. The catalysts were prepared by three different methods: incipient wetness impregnation (Cu/SiO_2-I and Cu/Al_2O_3-I), precipitation–deposition (Cu/SiO_2-PD) and co-precipitation (CuMgAl and CuZnAl). After the thermal treatment, the samples were characterized by X-ray diffraction (XRD) and temperature-programmed reduction (TPR). Only a tenorite-like polycrystalline phase, formed by large CuO crystallites, was identified in Cu/SiO_2-I, while none crystalline phase was observed in the case of Cu/SiO_2-PD. Instead, a unique spinel-like phase was detected with Cu/Al_2O_3-I, CuMgAl and CuZnAl. Combining XRD and TPR results, we concluded that Cu^{2+} is highly dispersed in the Cu/SiO_2-PD, Cu/Al_2O_3-I, CuMgAl and CuZnAl calcined precursors. As a consequence, after reduction in H_2 flow, the metal dispersion and hydrogen chemisorption capacity of these four samples were one order higher than for Cu/SiO_2-I. The catalytic tests showed that Cu/SiO_2-PD was not only the most active but also the most selective and stable catalyst of these series: a D-fructose conversion of around 100% was reached after 6 h reaction, with a selectivity to D-mannitol of around 78–80%. These results show that selective hydrogenation of fructose to D-mannitol is favoured over metal Cu nanoparticles dispersed on the surface of a neutral support as SiO_2. Additional catalytic tests, varying fructose initial concentration (0.028–0.220 M) and hydrogen pressure (20–40 bar), were carried out with Cu/SiO_2-PD. A zero reaction order respect to D-fructose and a second reaction order respect to H_2 were estimated. In addition, it was found that D-mannitol selectivity is not dependent on reactant initial concentration and hydrogen pressure.

* Corresponding author.
E-mail address: amarchi@fiq.unl.edu.ar (A.J. Marchi).

http://dx.doi.org/10.1016/j.cej.2017.02.127
1385-8947/

1. Introduction

Since the world's fossil fuel resources are decreasing and due to the effect of gas emission on the climate changes of our planet, the chemical industry seeks to replace these non-renewable raw materials by others coming from renewable sources. Undoubtedly, biomass is one of the most attractive renewable sources available on our planet. In particular, carbohydrates constitute the two thirds of the biomass and they are adequate for obtaining many useful chemicals. Therefore, they are expected to be a major feedstock for the chemical industry and especially for fine chemicals synthesis [1].

Over the recent years, the interest towards carbohydrates-derived products, such as sugar alcohols, has grown considerably owing to diversified applications in medical treatments, foodstuffs, cosmetics and pharmaceuticals [2–5]. D-mannitol is a low-caloric sweetener, thus its main application is in the food industry as sweetener. Furthermore, it is non-hygroscopic and the least water-soluble sugar alcohol of all of the commercially available, which favor its purification by crystallization processes. As well, it is employed for the production of mannitol hexanitrate, which is used as vasodilator in hypertension treatments [6], and in the chemical synthesis of other high added value compounds, such as propanediol [7,8].

D-mannitol is present in many plants such as manna, seaweed and algae. However the extraction of D-mannitol from these raw materials is not a profitable process. Instead, fermentation [9] and catalytic hydrogenation processes [10] are used industrially. Particularly, the catalytic hydrogenation process has been widely used for the commercial production of D-mannitol. Nowadays, mannitol can be obtained by catalytic hydrogenation of monosaccharides like fructose (Fig. 1) or from glucose-fructose mixtures, using Raney-Ni as catalyst. Higher yields in mannitol are achieved with pure fructose or syrups with high fructose concentration than from a glucose-fructose mixture. However, with Ni-based catalyst, only about half of the fructose is hydrogenated to mannitol while the other half is converted to sorbitol [8,11,12]. This results in low yield and selectivity to mannitol (45–50%). Carbon supported noble metal catalysts, such as Ru and Pt, were reported as the most active in the hydrogenation of carbohydrates [4,13]. However, these metals are expensive and give low yield and selectivity to mannitol, similar to those reached with nickel-based catalysts, i.e., around 50% [14–16]. Copper-based catalysts were less active, but more selective to mannitol than the noble and nickel-based ones. At best, the yield in D-mannitol was close to 67% when these Cu-based catalysts were used in the liquid-phase hydrogenation of D-fructose [17–19]. For example, selectivity to mannitol around 66% was obtained over $Cu/ZnO/Al_2O_3$ and Cu/SiO_2 catalysts [20]. Therefore, the nature of the metal and the support, as well as the preparation method, can play an important role in the selective hydrogenation of D-fructose to D-mannitol.

D-mannitol yields over 70% were only achieved when co-catalysts, in conjunction with Cu/SiO_2 catalysts, were employed to hydrogenate sugars. The best results were obtained when borates were used as co-catalysts. In previous works, a cyclic compound between sugar and borate, with a β–furanose-like form, was assumed to be preferentially formed when borate co-catalysts were added into an aqueous D-fructose solution. This cyclic compound, at difference of α–furanose-like intermediates, can be selectively hydrogenated to D-mannitol [19,21]. However, the co-catalysts are added to the liquid phase and therefore its separation from the products could become a difficult task in industrial processes. The best results were obtained when borates are used as co-catalysts, but borate-sugar esters are formed in liquid phase what makes very difficult the separation of the co-catalyst from the poliols obtained by hydrogenation [19,21,22]. Thus, it is of great interest to develop Cu-based catalysts to achieve mannitol yields higher than 70% without employing co-catalysts.

In this work, Cu-based catalysts, prepared by different methods and using different oxides as supports, were evaluated in the liquid-phase hydrogenation of D-fructose to determine the influence of the physicochemical and structural properties on the catalyst activity, the stability and the selectivity to D-mannitol. The objective is to determine the feasibility of improving the yield and selectivity to D-mannitol, previously reported in the liquid-phase hydrogenation of fructose, by employing new highly dispersed metal Cu catalysts without using a co-catalysts.

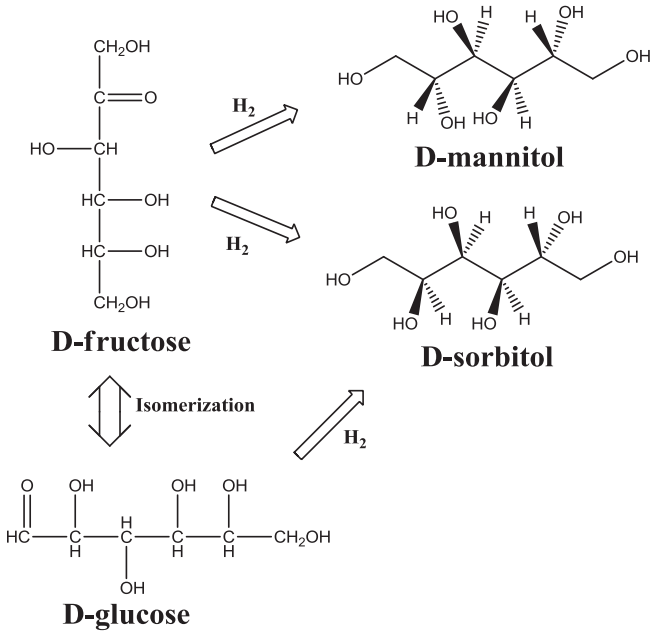

Fig. 1. Reaction scheme for hydrogenation of fructose in liquid phase.

2. Experimental

2.1. Catalyst preparation

The Cu/SiO_2-I and Cu/Al_2O_3-I catalyst precursors were prepared using the incipient wetness impregnation method by adding dropwise an aqueous solution of $Cu(NO_3)_2{\cdot}3H_2O$ (Merck 98%), with the suitable concentration, over commercial SiO_2 (Sigma-Aldrich, 230 m^2/g) and γ-Al_2O_3 (Ketjen CK 300, 190 m^2/g), respectively. The samples obtained in this way were dried in an oven at 373 K for 12 h, and finally calcined in air flow at 673 K for 2 h.

The Cu/SiO_2-PD catalyst was prepared by the precipitation-deposition method by adding simultaneously aqueous solutions of $Cu(NO_3)_2{\cdot}3H_2O$ and K_2CO_3 into an aqueous silica suspension, placed in a stirred glass reactor, while the pH was maintained at 7.2 ± 0.2, i.e. above the isoelectric point of the silica, and the temperature at 338 K. The precipitate was separated by filtration, washed with deionized water and dried at 358 K overnight. Finally, the hydrated precursor thus obtained was calcined in air flow at 673 K for 2 h.

The hydrated precursors of CuMgAl and CuZnAl were prepared by the co-precipitation method at 338 K, keeping the pH at7.2 ± 0.2 for CuZnAl and at 10.0 ± 0.2 in the case of CuMgAl, following the procedures described elsewhere [23–26]. The precipitates obtained in these conditions were filtrated, washed with deionized water at 338 K and dried at 353 K overnight. These hydrated precursors

were thermally decomposed in N_2 flow at 773 K for 5 h to obtain the corresponding mixed oxides.

2.2. Catalyst characterization

Elemental composition of the calcined samples were determined by atomic absorption spectroscopy (AAS) using a Perkin-Elmer 3110 spectrometer. The specific surface area (*Sg*) and pore volume (*Vg*) of the samples were measured by N_2 physisorption at 77 K in a Quantachrome Autosorb I sorptometer.

The identification of polycrystalline species in the oxide precursors were carried out by X-ray diffraction (XRD) employing a Shimadzu XD-1 diffractometer, with Ni-filtered Cu-Kα radiation (λ = 0.1540 nm) and 2°.min^{-1} speed scan. The average crystallite size was estimated applying Scherrer's equation. Temperature programmed reduction (TPR) profiles of the oxide precursors were obtained in H_2(5%)/Ar flow (60 cm^3.min^{-1}) using a Micromeritics Auto Chem 2920 system equipped with TCD detector.

The Cu metal dispersion was determined by pulse titration with N_2O at 363 K and considering a Cu_S^0/N_2O stoichiometry of 2, where Cu_S^0 indicates the superficial atoms of metal copper [27]. The reactor effluent during titration was analyzed by mass spectroscopy (MS) using a Balzers Omnistar unit. Previously to titration, the samples were reduced in-situ at 573 K by flowing H_2 (100%) through the reactor.

Electron microscopy observations were carried out at the LMA-INA-UNIZAR facilities using a Tecnai G2-F30 Field Emission Gun microscope with a super-twin lens and 0.2 nm point-to-point resolution and 0.1 line resolution operated at 300 kV. Energy dispersive X-ray spectroscopy (EDS) analysis and high angle annular dark field scanning transmission electron microscopy images (HAADF-STEM) were performed to determine the location and composition of Cu nanoparticles. HAADF detector enables to acquire HAADF-STEM images with atomic number contrast for high scattering angles of the electrons (Z-contrast). To prepare the samples for electron microscopy observation, catalyst powder was dispersed in milli-Q water. After 30 s in an ultrasonic bath, a drop of this suspension was applied to a Nickel grid (200 mesh) coated with carbon film, and allowed to dry in air. Histograms were obtained by measuring the particle size in STEM-HAADF images using a TEM Imaging & Analysis Offline FEI software. The samples analyzed by TEM were previously reduced in H_2 flow for 2 h at 823 K and then passivated in O_2 (2%)/N_2 for 20 min at room temperature to avoid the bulk oxidation of the samples.

Hydrogen chemisorption was measured via volumetric adsorption experiments in the pressure range 0–0.15 bar applying the double isotherm method, as described elsewhere [24]. The samples were reduced in-situ with H_2 (100%) at 573 K for 2 h, and then evacuated at 10^{-7} bar for 2 h. The amount of chemisorbed hydrogen was calculated as the difference between the total and the physisorbed H_2.

The concentration and acidity of surface acid sites was determined by temperature-programmed desorption of NH_3 (NH_3-TPD). Firstly, the samples (100 mg) were heated in He (60 cm^3.min^{-1}) flow from 298 K to 573 K at 10 K.min^{-1} and kept at 573 K for 1 h. Afterwards, the samples were cooled down to 373 K and exposed to an NH_3(1%)/He gaseous stream for 1 h. The physisorbed NH_3 was removed by flowing He (60 cm^3.min^{-1}) at 373 K for 0.5 h. Finally, the temperature was raised from 373 K to 973 K at 10 K.min^{-1} and the NH_3 concentration in the effluent was measured by mass spectrometry (MS) using a Balzers Omnistar unit.

The concentration and basicity of surface basic sites were determined by temperature-programmed desorption of CO_2 (CO_2-TPD). Firstly, the samples (50 mg) were pretreated by heating from 298 K to 573 K in N_2 flow (60 cm^3.min^{-1}) at 10 K.min^{-1}. The final temperature was kept for 1 h. Then, the system was cooled down to room temperature and the samples were exposed to a CO_2(2%)/N_2 gas stream (60 cm^3.min^{-1}) until surface saturation. Finally, the temperature was increased from 298 K to 1073 K in N_2 (60 cm^3.min^{-1}) flow at 10 K.min^{-1}. The effluent gas was converted to CH_4 at 400 °C in a reactor loaded with Ni/Kieselghur catalyst, while passing H_2 flow, and then analyzed by an on-line Gas Chromatograph SRI 310C using a flame ionization detector (FID).

2.3. Catalytic tests

The liquid-phase catalytic hydrogenation of D-fructose (Anedra 99.9%) was carried out in a 500 cm^3 stainless steel autoclave at 373 K and 20–40 bar of H_2 pressure, using 150 cm^3 of a mixture of ethanol/deionized water (70:30% vol.) as solvent. Prior to the catalytic tests, the samples (0.5 g) were activated ex-situ in H_2 (100%) flow (60 cm^3.min^{-1}) for 2 h at 523–573 K. Then, the reduced samples were transferred under inert atmosphere (N_2) to the high-pressure reactor containing a solution of fructose (0.028–0.22 M) in ethanol/water. Afterwards, the reaction system was stirred at 760 rpm and heated up to the reaction temperature at 5 K.min^{-1}. Finally, when the reaction temperature was reached, the total pressure was augmented to the preset H_2 pressure value.

Liquid samples were withdrawn from the reactor every 15–30 min so that less than a 3% of the total liquid volume was extracted during the complete run. Off-line analysis of the reaction mixtures were done with a HPLC Shimadzu modular system equipped with a dual-pump, a fixed-loop (20 μL) injector and a temperature controlled oven. The separation of reactants and product was performed using a Phenomenex column (Phenosphere 5 micras, NH_2, 80Å, 250 mm × 4.60 mm) and the detection and quantification by means of a differential refractive index detector (RID-10A). The injected samples were eluted using acetonitrile-water (85:15) as mobile phase at 0.8 cm^3.min^{-1} and 298 K. All solvents were HPLC grade and the water was ultrapurified by reverse osmosis employing an OSMOION equipment. The mobile phase was previously filtrated through a 0.22 μm nylon filter. In all of the cases, the only compounds detected and quantified were fructose, glucose, sorbitol and mannitol.

The fructose conversion was calculated as $X_F = (n_F^0 - n_F)/n_F^0$, where n_F^0 are the initial fructose moles and n_F are the fructose moles at a given reaction time. The product yields (ηj) were calculated as $\eta j = \nu_F.n_j/\nu_j.\ n_F^0$, where n_j is the moles of product j and ν_F and ν_j are the stoichiometric factors of fructose and product j, respectively. Selectivity to product j (S_j) was obtained as $Sj = \eta_j/\sum\eta_i$, where η_i is the yield in each product. The carbon balance (CB) was defined as $CB = (\alpha_F \cdot n_F + \alpha_M \cdot n_M + \alpha_S \cdot n_S + \alpha_G \cdot n_G)/\alpha_F \cdot n_F^0$, where α_F, α_M, α_S and α_G are the number of carbon atoms in fructose, mannitol, sorbitol and glucose, which is 6 in all of the cases. Thus, the last expression for *CB* simplifies to $CB = (n_F + n_M + n_S + n_G)/n_F^0$. The initial rates of fructose conversion (r_F^0, mol of fructose .h^{-1}.g$_{Cat}^{-1}$) were estimated by applying polynomial differentiation on the conversion data as a function of $W.t/n_F^0$ and evaluating the corresponding derivative at zero time.

3. Results and discussion

3.1. Sample characterization

The results obtained from the characterizations performed on the samples used in this work are summarized in Table 1. The Cu load in the Cu/Al_2O_3-I, Cu/SiO_2-I, Cu/SiO_2-PD and CuZnAl samples were between 8 and 13%, while for the CuMgAl sample was 18 wt%. The specific surface area (Sg) of Cu/SiO_2-I, Cu/SiO_2-PD and Cu/Al_2O_3-I were slightly lower than the calcined SiO_2 (230 m^2.

Table 1
Physicochemical characterizations of the Cu-based catalysts.

Sample	Cu[a] (wt.%)	Sg ($m^2.g^{-1}$)	TPR[b] T_M (K)	V_{HI}[c] ($cm^3.g^{-1}$)	D_{Cu}[d] (%)	L[e] (nm)	CO_2-TPD		NH_3-TPD	
							n_b[g] ($\mu mol.g^{-1}$)	T_M[f] (K)	n_a[h] ($\mu mol.g^{-1}$)	T_M[f] (K)
Cu/SiO_2-I	11.4	221	563	0.016	2	32	nd	–	nd	–
Cu/SiO_2-PD	11.3	225	513	0.144	21	3,3	nd	–	4	493
Cu/Al_2O_3-I	8.0	175	533	0.170	16	6,5	35	395	20	475
CuZnAl	12.9	171	523	0.242	22	–	210	405	nd	–
CuMgAl	17.9	291	473	0.289	11	–	420	430	192	673

[a] Cu content determined by Atomic Absorption Spectroscopy.
[b] Temperature at the maximum H_2 consumption in TPR experiments.
[c] Volume of irreversibly chemisorbed hydrogen per gram of metallic Cu.
[d] Metallic Cu dispersion determined by titration with N_2O at 363 K.
[e] Cu metal particle size estimated from the metallic dispersion assuming cubic geometry.
[f] Temperature at the maximum desorption rate.
[g] Basic site concentration determined by TPD of CO_2.
[h] Acid site concentration determined by TPD of NH_3.

g^{-1}) and γ-Al_2O_3 (190 $m^2.g^{-1}$), indicating that textural properties of the support were not significantly affected during the sample preparation (Table 1). The specific surface areas of the mixed oxides obtained by the co-precipitation method at constant pH were 171 $m^2.g^{-1}$ for CuZnAl and 291 $m^2.g^{-1}$for CuMgAl, the latter being the sample with the largest specific surface area among all the samples prepared in this work.

The X-ray diffraction patterns of the oxide precursors obtained after thermal decomposition, either in air o N_2, are shown in Fig. 2. A polycrystalline phase, with a tenorite-like structure (CuO, JCPDS 5-0661) and a mean crystallite size of about 32 nm, estimated by applying the Scherrer's equation, was detected in the case of Cu/SiO_2-I oxide precursor. Instead, only the amorphous halo diffraction, characteristic of SiO_2, was observed for the Cu/SiO_2-PD calcined precursor. This is suggesting that the copper oxide phase obtained by thermal decomposition is quasi-amorphous or the crystal domains are smaller than 4 nm. In the case of Cu/Al_2O_3-I, CuZnAl and CuMgAl samples, only broad peaks matching a polycrystalline phase with a spinel-like structure (γ-Al_2O_3: JCPDS 10-425, $ZnAl_2O_4$: JCPDS 5-0669 and $MgAl_2O_4$: JCPDS21-1152) were detected. As in the case of Cu/SiO_2-PD, no polycrystalline CuO was detected. Furthermore, for the mixed oxide samples obtained by the co-precipitation method, no ZnO or MgO segregation was observed. Then, it is very likely that Zn^{2+} and Mg^{2+}cations in excess remains highly dispersed in the spinel-like matrix [23].

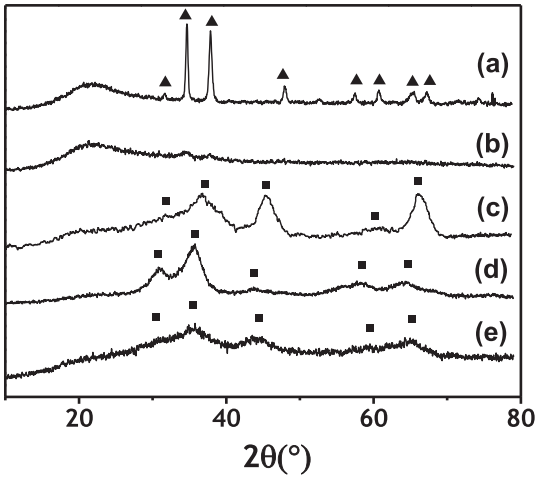

Fig. 2. X-ray diffractograms of samples thermally treated at 673–773 K under gas flow: (a) Cu/SiO_2-I, (b) Cu/SiO_2-PD, (c) Cu/Al_2O_3-I, (d) CuZnAl, (e) CuMgAl. ▲CuO, ■ spinel-like phase.

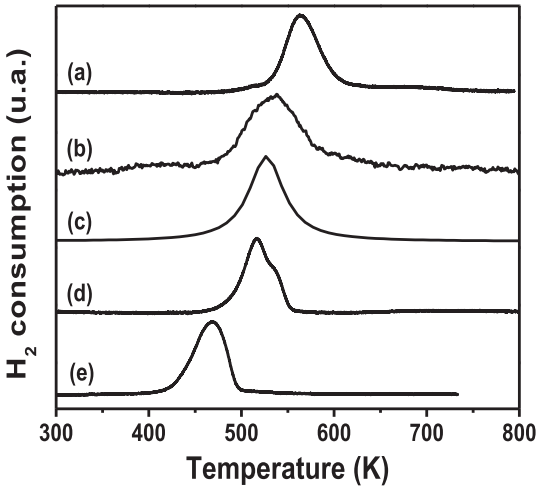

Fig. 3. TPR profiles [H_2 (5%)/Ar; 60 $cm^3.min^{-1}$; 10 $K.min^{-1}$]: (a) Cu/SiO_2-I, (b) Cu/Al_2O_3-I, (c) CuZnAl, (d) Cu/SiO_2-PD, (e) CuMgAl.

Only one H_2 consumption peak was observed in all of the TPR profiles of the oxide precursors (Fig. 3). The temperatures at the maximum H_2 consumption (T_{MAX}) are summarized in Table 1. These values indicate that the reducibility of the oxidized copper species present on these precursors followed the trend: Cu/SiO_2-I < Cu/Al_2O_3-I < CuZnAl < Cu/SiO_2-PD < CuMgAl. In a previous work, we concluded that the reducibility of copper oxide species augments as particle size diminishes due to increasing Cu-support interaction [23]. Consequently, the lowest reducibility of Cu/SiO_2-I can be explained assuming the reduction of large CuO particles with tenorite-like structure that have very low or none interaction with SiO_2. Reducibility of Cu/SiO_2-PD precursor is higher than that one of Cu/SiO_2-I, probably due to the smaller particles of oxidized copper species interacting with support surface after calcination. In summary, the observed reducibility pattern may be explained on the basis of the particle sizes of the copper species formed after calcination and their interaction with the support (Fig. 3 and Table 1). Besides, no H_2 consumption peak due to $CuAl_2O_4$ reduction was detected in the TPR profiles of CuZnAl and CuMgAl, which is consistent with XRD characterization results. In addition, in all of the samples, these TPR profiles indicate that oxidized copper species were completely reduced under the conditions of activation employed for the catalytic tests.

The metallic Cu dispersion (D_{Cu}) was determined by N_2O decomposition, after reduction in H_2 (100%) flow at 300 °C (Table 1). The highest values for Cu dispersion were reached for Cu/SiO_2-PD (21%) and CuZnAl (22%), which is twice higher than

that one for CuMgAl sample (11%). Cu/Al_2O_3-I exhibited an intermediate metal dispersion (16%) in the series of catalysts studied. The dispersion for the impregnated sample on SiO_2, Cu/SiO_2-I, was one order of magnitude lower than those of the preceding samples. The pattern for the metallic copper dispersion, in the catalyst series used in this work, was: CuZnAl ≅ Cu/SiO_2-PD > Cu/Al_2O_3-I > CuMgAl ≫ Cu/SiO_2-I. Dispersion values of metallic copper allowed the estimation of the average particle size of Cu/SiO_2-I, Cu/SiO_2-PD and Cu/Al_2O_3-I, assuming cubic metal particles and using a surface density of Cu atoms of 1.08×10^{-15} at.cm^{-2} (Table 1).

One of the samples with the highest dispersion, Cu/SiO_2-PD, was also observed by TEM and the main results are presented in Fig. 4. The HAADF-STEM images show that the metallic copper phase is highly dispersed on the support surface and it is mainly composed by nanoparticles with less than 10 nm in size (Fig. 4A and C). The energy dispersive X-ray spectroscopy (EDS) analysis confirmed that the observed nanoparticles are of copper (Fig. 4B). By counting around 60 metallic copper nanoparticles, the histogram shown in Fig. 4C was obtained: it was determined that most of these nanoparticles are between 3 and 4 nm. The estimated mean size was 4.7 nm and the median was 3.8 nm. Similar distributions for the metal copper nanoparticles were observed on other catalyst particles of the dispersed powder sample. All these results are in a good agreement with the mean size determined by titration with N_2O (Table 1), thus confirming that the metallic phase on Cu/SiO2-PD is formed by nanoparticles having mostly less than 5 nm in size.

The significant difference of the metallic dispersion values observed with Cu/SiO_2-PD catalyst regarding Cu/SiO_2–I was attributed to the preparation method. The constant pH (7.2 ± 0.2) used in this work for the precipitation-deposition, which was significantly higher than the isoelectric point of the silica (pH = 1–2), played a very important role on the metallic dispersion of copper in the final Cu/SiO_2-PD catalysts. Under these conditions, SiO_2 surface has a very high negative charge density, i.e., there are a lot of negative surface centers on which Cu^{2+} ions can be adsorbed. Thus, a great number of nuclei are initially formed, on which nanoparticles of hydrated precursor can be developed. As a consequence, a highly dispersed phase containing Cu^{2+} ions can be deposited on the support surface, with a relatively high Cu-SiO_2 interaction. After calcination in air flow and reduction in H_2 flow, this Cu-SiO_2 interaction favors the formation of a highly dispersed metallic copper phase. Dewing et al. [18] also prepared Cu/SiO_2 catalysts by the precipitation-deposition method, but these catalysts were prepared at variable pH and using ammonium compounds as precipitating reagents. In this case, the average size of the metal copper particles was around 25 nm, i.e. five to six times larger than the ones formed in our Cu/SiO_2-PD catalyst. This result shows that, during the precipitation-deposition process, the pH has an important influence on the surface properties of the catalyst.

The irreversible H_2 chemisorption capacity per gram of Cu for the reduced samples followed the trend: CuMgAl > CuZnAl > Cu/Al_2O_3-I > Cu/SiO_2-PD > Cu/SiO_2-I (Table 1). Therefore, CuMgAl is the sample with the highest reducibility and capacity for H_2 chemisorption, while Cu/SiO_2-I has the lowest ones. Instead, Cu/SiO_2-PD, Cu/Al_2O_3-I and CuZnAl, showed and intermediate behavior.

The acid and basic properties of the calcined samples were determined by NH_3-TPD and CO_2-TPD, respectively. The main results are summarized in Table 1. None surface acid or basic sites were detected for Cu/SiO_2-I sample, while only a very small amount of surface acid sites were observed on Cu/SiO_2-PD. In contrast, both acid and basic sites were observed on the surface of Cu/Al_2O_3-I and CuMgAl samples. In the case of CuZnAl sample, some surface basicity was observed but none surface acid sites were detected. The concentration of surface acid sites followed the pattern: CuMgAl ≫ Cu/Al_2O_3-I ≫ Cu/SiO_2-PD. Furthermore, taking into account the temperature at the maximum NH_3 desorption rate (T_M), CuMgAl showed the highest surface acidity of this sample series. On the other hand, the pattern for the concentration of surface basic sites was: CuMgAl > CuZnAl > Cu/Al_2O_3-I. In this case, the CO_2 desorption temperature was similar for the three samples, indicating no significant differences among the surface basicity of them.

3.2. Catalytic tests

3.2.1. Activity of Cu-based catalyst and product distribution

The evolution of D-fructose conversion as a function of time is shown in Fig. 5A. All catalysts are active for the fructose hydrogenation, but the evolution of the reactant conversion was rather different for each one. The fructose conversions (X_F) after 6 h of reaction are shown in Table 2: almost 100% conversion was reached only with Cu/SiO_2-PD, while the lowest conversion

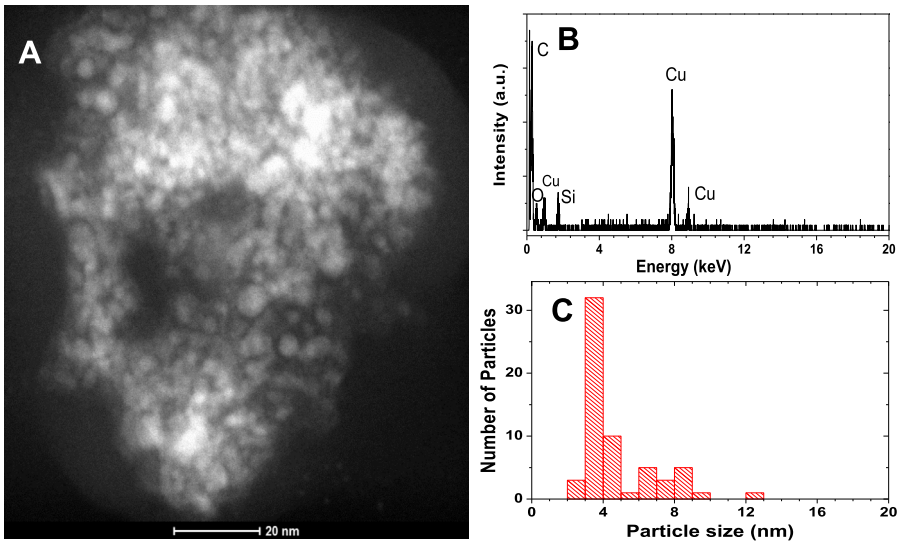

Fig. 4. STEM-EDS of reduced and passivated Cu/SiO_2-PD sample, prepared by the precipitation-deposition method at pH = 7.2 ± 0.2: (A) HAADF-STEM image; (B) Energy Dispersive X-ray Spectroscopy (EDS) analysis; (C) Size distribution of metallic copper particles.

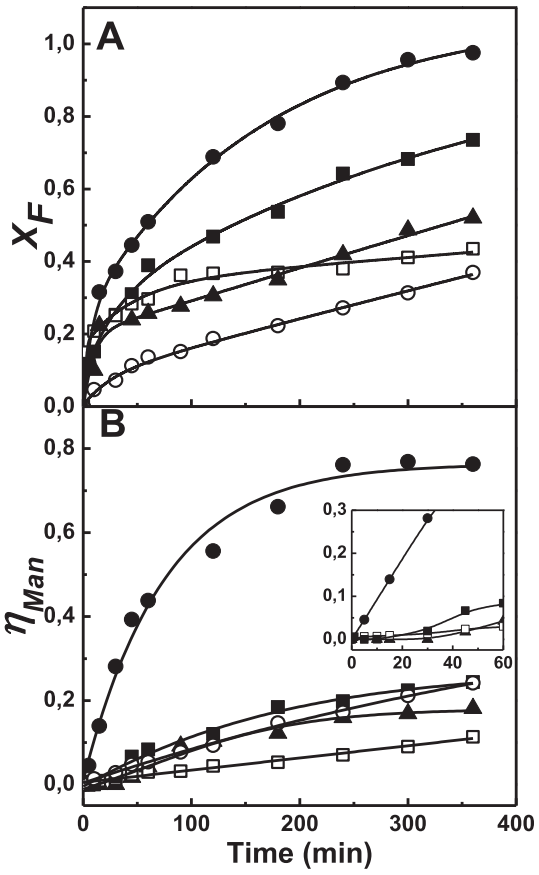

Fig. 5. Performance of Cu-based catalysts in the liquid-phase hydrogenation of fructose at T = 373 K, p_{H2} = 40 bar, C_F^0 = 0.055 M: ○ Cu/SiO_2-I, ● Cu/SiO_2-PD, ▲ Cu/Al_2O_3-I, □ CuZnAl, ■ CuMgAl. (A) Fructose conversion (X_F) and (B) mannitol yield (η_M) as a function of reaction time.

(X_F = 37%) was obtained with Cu/SiO_2-I. The fructose conversion with Cu/Al_2O_3-I, CuZnAl and CuMgAl increased rapidly in the first 30 min of reaction, but then the rate of reactant conversion diminished drastically. The most striking decrease for the rate of fructose conversion was observed with CuZnAl catalyst. Thus, the final conversion was around 75% with CuMgAl, 52% with Cu/Al_2O_3-I and 40% with CuZnAl. In summary, the conversion pattern after 6 h reaction was the following: Cu/SiO_2-PD > CuMgAl > Cu/Al_2O_3-I > CuZnAl > Cu/SiO_2-I.

It is important to notice that, although the fructose conversion increases with time during the first 30 min, in general, there is not a good correlation with the formation rate of the major reaction products, i.e., mannitol and sorbitol (Fig. 5A and B). The yield in mannitol with Cu/Al_2O_3-I, CuZnAl y CuMgAl catalysts was practically zero at the beginning of the reaction and polyol formation was observed only after 25–30 min (inset in Fig. 5B). A similar evolution was observed for sorbitol (not shown in this figure). These evolutions for the initial yields in the corresponding polyols are not in accordance with the rapid disappearance of fructose observed with these catalysts (Fig. 5A). It is worth to notice that this induction period in the production of mannitol and sorbitol was not observed with Cu/SiO_2-PD and Cu/SiO_2-I. In addition, it was verified that there is good agreement between the evolutions of the fructose conversion and the total yield in the two polyols when the metallic copper was supported on silica.

In order to find an explanation for the above differences, the carbon balance was analyzed. Fig. 6 shows the carbon balance (CB) as a function of the reaction time for all of the catalysts used in this work. The CB for Cu/SiO_2-PD and Cu/SiO_2-I reached values between 95% and 98%, while the CB for the rest of the catalysts decreased rapidly during the first minutes to 80–75%. These evolutions suggest that it is very likely that fructose and/or some of the hydrogenation products initially formed were strongly adsorbed on the surface of Cu/Al_2O_3-I, CuZnAl and CuMgAl. In the order to verify this hypothesis, additional experiments were carried out at the same conditions of the hydrogenation experiments, but in an inert atmosphere (N_2), i.e. in the absence of H_2. Fig. 7 shows the fructose molar concentration (C_F^0) as a function of time after addition of this carbohydrate to the system. It was verified that, with CuMgAl, CuZnAl and Cu/Al_2O_3-I catalysts, the fructose concentration diminished with the contact time. A very fast drop of the fructose concentration was observed with CuMgAl in the first minutes and afterwards the decrease is much slower. The evolutions were similar for CuZnAl and Cu/Al_2O_3-I, but the initial decrease of the fructose concentration was less dramatic than in the case of CuMgAl. Instead, fructose disappearance with silica-supported Cu catalysts was negligible and fructose concentration practically kept constant during all the experiment.

These results are in agreement with the hypothesis that the disappearance of fructose during the first 30 min of reaction with CuMgAl, CuZnAl y Cu/Al_2O_3-I is due to the strong adsorption of reactant over the surface of these three catalysts. This fact can be

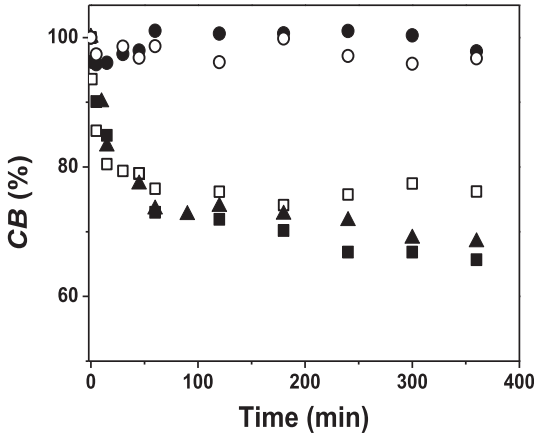

Fig. 6. Carbon balance (CB) as a function of reaction time. ○ Cu/SiO_2-I, ● Cu/SiO_2-PD, ▲ Cu/Al_2O_3-I, □ CuZnAl, ■ CuMgAl.

Table 2
Initial rates for product formation (r_P^0), fructose conversion (X_F), selectivity (Sj) and carbon balance (CB) after 6 h of reaction in the liquid-phase hydrogenation of fructose over Cu-based catalysts.

Catalysts	r_P^0 x 10^2 (mol.h^{-1}.g^{-1})	X_F (%)	S_M (%)	S_S (%)	S_G (%)	CB (%)
Cu/SiO_2-I	0.22	37	68	28	–	96
Cu/SiO_2-PD	2.28	98	78	22	–	98
Cu/Al_2O_3-I	0.15	52	68	29	–	69
CuZnAl	0.04	41	43	14	43	78
CuMgAl	0.28	74	64	18	18	66

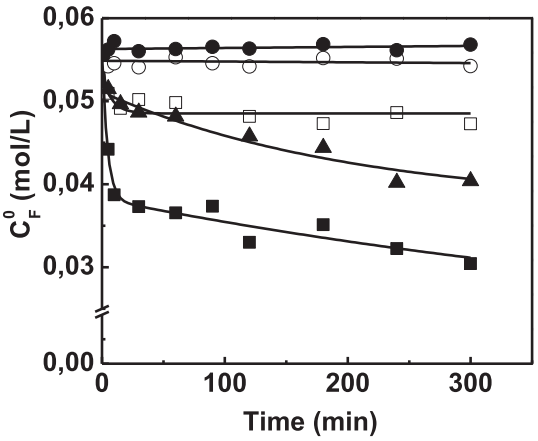

Fig. 7. Evolution of fructose concentration as a function of time over Cu-based catalysts in absence of H_2 at T = 373 K, P_{N2} = 40 bar and C_F^0 = 0.055 M: ○ Cu/SiO_2-I, ● Cu/SiO_2-PD, ▲ Cu/Al_2O_3-I, □ CuZnAl, ■ CuMgAl.

explained considering the initial interaction of fructose with acid and basic sites present on the surface of the Al_2O_3 and mixed oxides of Mg-Al and Zn-Al, which are not present on the SiO_2 surface (Table 1). These strongly adsorbed fructose molecules cannot be easily hydrogenated, what may explain the disappearance of fructose without production of polyols.

The initial rates for the production of mannitol and sorbitol (r_P^0, $mol.h^{-1}.g_{cat}^{-1}$) are presented in Table 2. For Cu/SiO_2-PD and Cu/SiO_2-I, the initial rates were estimated at time equal to zero, since no induction time in the product formation was observed with these two catalysts. Instead, for Cu/Al_2O_3-I, CuZnAl y CuMgAl, the initial rates were calculated after correction of the induction time. The r_P^0 with Cu/SiO_2-PD catalyst was at least one order of magnitude higher than with the other catalysts (Table 2). The highest catalytic activity of Cu/SiO_2-PD can be attributed to metal copper nanoparticles (3–4 nm) highly dispersed over a neutral support (SiO_2), which have a relatively high H_2 chemisorption capacity. Instead, in the case of Cu/SiO_2-I, the metal phase is constituted by large particles of metallic copper (>30 nm) with low capacity for H_2 chemisorption (Table 1). The low hydrogenation rates observed with Cu/Al_2O_3-I, CuMgAl and CuZnAl, in spite of their high metallic dispersion and high H_2 chemisorption capacity, may be explained considering a very strong adsorption of fructose over the surface acid and/or basic sites that are neighboured to the metallic sites. The strongly adsorbed fructose must be partially blocking the active sites of these catalysts, thus making difficult the adsorption and dissociation of H_2, and therefore the subsequent hydrogenation of reactant molecules. Evidence of the strong adsorption of fructose over Cu/Al_2O_3-I, CuZnAl and CuMgAl was obtained experimentally in this work and shown in Figs. 6 and 7.

Regarding the product distribution, mannitol and sorbitol were observed with all of the catalysts, while glucose was detected only with CuZnAl and CuMgAl catalysts. Cu/SiO_2-PD was the catalyst with the highest yield in D-mannitol ($\eta_M \cong 76\%$), after 6 h reaction (Fig. 5B). It is worth noting, that D-mannitol yield achieved with Cu/SiO_2-PD was even higher than the values reported in previous works, in which Cu-based solid catalysts without a co-catalyst were employed for the D-fructose hydrogenation in liquid phase. At the same time on reaction, the mannitol yield with Cu/SiO_2-I and CuMgAl catalysts was only 25%, while it was lower than 20% with Cu/Al_2O_3-I and CuZnAl. In summary, the yield in mannitol (η_M) followed the trend: Cu/SiO_2-PD > Cu/SiO_2-I ≅ CuMgAl > Cu/Al_2O_3-I > CuZnAl (Fig. 5B). Then, Cu/SiO_2-PD was the catalyst with the highest activity and selectivity to D-mannitol of these series ($S_M \cong 78\%$, Table 2). In previous works, similar selectivity could be obtained with Cu-based catalysts only if a co-catalyst was employed [19,21]. The selectivity reached with Cu/SiO_2-I and Cu/Al_2O_3-I was 68% at 6 h reaction (Table 2), which is similar to those reported by Makkee et al. and Toukoniitty et al. [19,20]. It seems that the metal copper nanoparticles formed on Cu/SiO_2-PD, which are highly dispersed on an inert support, play a very important role in the selective hydrogenation of D-fructose to D-mannitol. Instead, large metal copper particles formed over the same support, as those in Cu/SiO_2-I, are less active for the selective hydrogenation of fructose to mannitol. In the case of the catalysts with spinel-like structure, constituted by small metal copper particles that are strongly interacting with amphoteric mixed oxides, the selectivity to D-mannitol was lower. This is because the basic and acid sites present on the surface of Mg-Al and Zn-Al catalysts favor the isomerization of D-fructose to D-glucose [28,29]. Strong adsorption of D-fructose over Cu/Al_2O_3-I was also observed but no formation of D-glucose occurs. This may be explained for low concentration of basic and acid sites on the Cu/Al_2O_3-I compared to co-precipitated catalysts (Table 1).

In summary, Cu/SiO_2-PD catalyst, in which the active phase is mainly constituted by nanoparticles of metallic copper over a support without surface acid and basic sites, is very active, selective and stable during hydrogenation of fructose in liquid phase, without using any kind of co-catalysts. Thus, a 100% fructose conversion and high values of yield and selectivity to D-mannitol, almost 80%, can be reached. On the other hand, Cu/SiO_2-I showed also low acidity and basicity, but it is constituted by large metal copper particles, which are much less active and selective for hydrogenation of fructose into D-mannitol than Cu/SiO_2-PD. In previous works, Cu/SiO_2 catalysts were also used for carbohydrates hydrogenation. However, selectivity to D-mannitol with these copper-based catalysts was always lower than 70%. Higher selectivities were reached only when borate co-catalysts were employed in conjunction with Cu/SiO_2 catalysts. In this work, we got similar activity and selectivity to D-mannitol, employing a Cu/SiO_2-PD catalyst, without any borate co-catalyst as used in previous works. We assume that some surface intermediates, probably with a similar β-furanose form as that observed by Makkee et al. [19], are preferentially formed on the surface of the metal Cu nanoparticles with 3–5 nm in size. These surface intermediates can be more easily and selectively hydrogenated into D-mannitol than those formed on the surface of larger metal copper particles. For example, it was suggested that an intermediate with α-furanose form is selectively converted into D-sorbitol instead of D-mannitol, while pyranose-like surface species are little reactive [7,19]. Thus, the highest activity and selectivity to D-mannitol of Cu/SiO_2-PD can be explained assuming that a most reactive surface intermediate, which can be preferentially hydrogenated into D-mannitol, is formed over 3–5 nm metal copper nanoparticles.

Based on the above results, a kinetic study with the most active, selective and stable Cu/SiO_2-PD catalyst was carried out. The aim is to estimate the reaction order respect to fructose and hydrogen for the conditions used in this work.

3.2.2. Influence of reactions conditions

The effect of initial fructose molar concentration (C_F^0) and hydrogen pressure (p_{H2}) on the activity of Cu/SiO_2-PD catalyst, at constant temperature, was also studied in this work. The order of reaction with respect to C_F^0 and p_{H2} was estimated using a pseudo-homogeneous kinetic model based on a power-law relationship between the initial reaction rate (r_F^0) and the initial concentrations of D-fructose (C_F^0) and partial hydrogen pressure (p_{H2}) in the liquid and gas phases, respectively (Eq. (1)).

$$r_F^0 = k(p_{H2})^{\alpha}(C_F^0)^{\beta} \quad (1)$$

Table 3
Initial hydrogenation rates (r_F^0), fructose conversion (X_F), selectivity (Sj) and carbon balance (CB) after 6 h of reaction in the liquid-phase hydrogenation of fructose over Cu/SiO_2-PD catalyst varying initial fructose concentrations and H_2 partial pressures.

C_F^0 (mol.l^{-1})	p_{H2} (bar)	$r_F^0 \times 10^2$ (mol.h^{-1}.g^{-1})	X_F %	S_M %	S_S %	S_G %	CB %
0.028		2.07	98	78	20	–	98
0.055	40	2.28	98	78	21	–	99
0.110		2.31	97	76	24	–	100
0.220		2.54	93	82	18	–	100
0.055	30	1.29	93	78	18	3	96
0.055	20	0.62	88	76	16	4	88

The dependence of the initial fructose hydrogenation rate (r_F^0) upon C_F^0 was studied at 383 K by varying C_F^0 between 0.028 and 0.22 M, while keeping constant p_{H2} at 40 bar. The plot representing ln r_F^0 as a function of ln C_F^0 is shown in Fig. 8(a). The reaction order with respect to C_F^0 (β) was estimated applying lineal regression with Eq. (1). With this procedure, the estimate for β was 0.09, what indicates that reaction is practically order zero respect to the fructose initial concentration. This result is indicating that fructose molecules adsorbs strongly on the active sites of Cu/SiO_2-PD catalyst, in agreement with results reported in this work (Figs. 5–7). In a similar study, Makkee et al. [19] carried out the hydrogenation of fructose over Cu(20%)/SiO_2 prepared by incipient wetness impregnation. They found that the reaction rate was first order respect to initial fructose concentration when C_F^0 <0.3 M. This reaction order is totally different to the one estimated in this work with a Cu/SiO_2 catalyst prepared by the precipitation-deposition method. The last is indicative that the interaction between fructose molecules and active surface of both catalysts is rather different. This supports the idea that the type of metal copper surface highly depends on the preparation method and plays an important role in the kinetic of fructose hydrogenation.

The fructose conversion and the selectivity to D-mannitol, sorbitol and D-glucose, for different initial concentrations of D-fructose and partial pressures of H_2, are shown in Table 3. At a H_2 partial pressure of 40 bar, the final fructose conversion was between 93 and 98% and the only products detected were always mannitol and sorbitol. In all of the cases, the selectivity to D-mannitol was around 80% and it was independent of fructose initial concentration.

The influence of hydrogen pressure was investigated varying p_{H2} between 20 and 40 bar at 383 K and C_F^0 = 0.055 M. A reaction order respect to H_2 (α) of 1.85 was estimated applying lineal regression with Eq. (1), at 0.055 M initial concentration of fructose (Fig. 8b). This estimate for parameter α indicates that fructose hydrogenation rate would be second order respect to H_2, which it is consistent with results obtained in a previous work [7]. Besides, at the same final reaction time, the fructose conversion fell down to 88% as the hydrogen pressure was diminished from 40 to 20 bar (Table 3). Instead, the mannitol selectivity was practically the same at H_2 pressures between 20 and 40 bar. However, at hydrogen partial pressures lower than 40 bar, some small amounts of glucose were detected, which becomes more difficult to be hydrogenated over non-noble metals catalyst as the H_2 partial pressure is diminished [7,15,19]. Besides, carbon balance also decreased as the hydrogen partial pressure was reduced (Table 3). This is probably due to the fact that the fructose and/or glucose strongly adsorbed on the metal copper surface is hydrogenated at lower rate when p_{H_2} <40 bar [4–7,11].

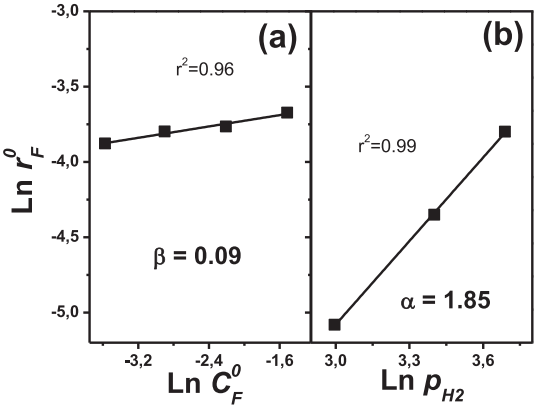

Fig. 8. Dependence of initial hydrogenation rate (r_F^0) with (a) initial fructose concentration [T = 373 K, p_{H2} = 40 bar] and (b) partial hydrogen pressure [T = 373 K, C_F^0 = 0.055 M] in the liquid-phase fructose hydrogenation over Cu/SiO_2-PD.

4. Conclusions

We have successfully achieved the selective hydrogenation of fructose in liquid phase with high yields in mannitol using a Cu-based catalyst supported over SiO_2, prepared by the precipitation-deposition method at constant pH, without using any co-catalyst. The high activity and selectivity to mannitol of this catalyst is attributed to active sites present on the surface of metallic copper nanoparticles, which are interacting with the surface of a support that have very low surface acidity and basicity, as SiO_2. The use of Cu catalyst with low metallic dispersion, such as Cu/SiO_2-I, prepared by the incipient wetness impregnation method, shows the lowest activity and selectivity to mannitol. An important loss of activity with time was observed when Cu is supported over metal oxides that have acid and basic surface sites, such as Al_2O_3 and Mg-Al or Zn-Al mixed oxides with a spinel-like crystalline structure. The last was explained assuming that strongly adsorbed fructose molecules blocks metal copper active sites during reaction. In addition, the basic and acid sites present on the surface of the mixed oxides promote the isomerization of fructose to glucose and, as a consequence, the yield in D-mannitol diminished. In summary, the metal copper nanoparticles must be highly dispersed on the surface of an inert support to reached high activity and selectivity to D-mannitol, since large metal copper particles or acid and basic sites on the support surface led to a drastic diminution of the selectivity to mannitol and hydrogenation activity of metal copper sites.

Acknowledgements

The authors thank the Universidad Nacional del Litoral (UNL), Consejo Nacional de Investigaciones Científicas y Técnicas (CONICET), and Agencia Nacional de Promoción Científica y Tecnológica (ANPCyT), Argentina, for the financial support and to LMA-INA-UNIZAR, Spain, for the transmission electronic microscopy analyses.

References

[1] A. Onda, T. Kajiyoshi, K. Yanagisawa, A new chemical process for catalytic conversion of D-glucose into lactic acid and gluconic acid, Appl. Catal. A Gen 343 (2008) 49–54.

[2] P. Imhof, J. Van der Waal, In: Catalytic Process Development for Renewable Materials, Wiley-Vch, Weinheim, Germany, 2013.

[3] F.W. Lichtenthaler, Unsaturated O- and N-heterocycles from carbohydrate feedstocks, Acc. Chem. Res. 35 (2002) 728–737.

[4] M. Ahmed, A. Kadhum, Hydrogenation of D-fructose over activated charcoal supported platinum catalyst, J. Taiwan Inst. Chem. Eng. 42 (2011) 114–119.

[5] H.L. Ohrem, E. Schornick, A. Kalivoda, R. Ognibene, Why is mannitol becoming more and more popular as a pharmaceutical excipient in solid dosage forms?, Pharm Dev. Technol. 1–6 (2016).

[6] S. Ghoreishi, R. Shahrestani, Innovative strategies for engineering mannitol production, Trends Food Sci. Technol. 20 (2009) 263–270.

[7] J. Kuusisto, J. Mikkola, P. Pérez Casal, H. Karhu, J. Väyrynen, T. Salmi, Kinetics of the catalytic hydrogenation of D-fructose over a CuO-ZnO catalyst, Chem. Eng. J. 115 (2005) 93–102.

[8] J. Zhang, S. Xu, S. Wu, Y. Liu, Hydrogenation of fructose over magnetic catalyst derived from hydrotalcite precursor, Chem. Eng. Sci. 99 (2013) 171–176.

[9] H. Ojamo, H. Koivikko, H. Heikkilä, Process for the Production of Mannitol by Immobilized Micro-Organisms, USP 2003 6,602,691B1.

[10] S.H. Song, C. Vieille, Recent advances in the biological production of mannitol, Appl. Microbiol. Biotechnol. 84 (2009) 55–62.

[11] A. Heinen, J. Peters, H. van Bekkum, The combined hydrolysis and hydrogenation of inulin catalyzed by bifunctional Ru/C, Carbohydr. Res. 330 (2001) 381–390.

[12] P. Vinkeand, H. van Bekkum, The dehydration of fructose towards 5 hydroxymethylfurfural using activated carbon as adsorbent, Starch 44 (1992) 90–96.

[13] E. Creeze, B.W. Hoffer, R.J. Berger, M. Makkee, F. Kaptejin, J.A. Moulijn, Three-phase hydrogenation of d -glucose over a carbon supported ruthenium catalyst – mass transfer and kinetics, Appl. Catal. A Gen. 251 (2003) 1–17.

[14] A. Heinen, G. Papadogianakis, R. Sheldon, J.A. Peters, H. van Bekkum, Factors effecting the hydrogenation of fructose with a water soluble Ru–TPPTS complex. A comparison between homogeneous and heterogeneous catalysis, J. Mol. Catal. A Chem. 142 (1999) 17–26.

[15] A. Heinen, J. Peters, H. van Bekkum, Hydrogenation of fructose on Ru/C catalysts, Carbohydr. Res. 328 (2000) 449–457.

[16] J. Wisniak, R. Simon, Hydrogenation of glucose, fructose, and their mixtures, Ind. Eng. Chem. Prod. Res. Dev. 18 (1979) 50–57.

[17] M.J. Climent, A. Corma, S. Iborra, Converting carbohydrates to bulk chemicals and fine chemicals over heterogeneous catalysts, Green Chem. 13 (2011) 520–540.

[18] J. Dewing, J.F. Ruddlesden, A. Stewart, D.J. Thompson, Process for Reduction of Sugar to Sugar-alcohols, EP 1980 0006313 A1.

[19] M. Makkee, A. Kieboom, H. Bekkum, Hydrogenation of D-fructose and D-fructose/D-glucose mixtures, Carbohydr. Res. 138 (1985) 225–236.

[20] B. Toukoniitty, J. Kuusisto, J.P. Mikkola, T. Salmi, D.Y. Murzin, Effect of ultrasound on catalytic hydrogenation of D-Fructose to D-mannitol, Ind. Eng. Chem. Res. 44 (2005) 9370–9375.

[21] M. Hegedus, S. Gobolos, J.L. Margitfalvi, M. Guisnet, Stereoselective hydrogenation of D-fructose to D-mannitol on skeletal and supported copper containing catalyst, Het. Catal. Fine Chem. 78 (1993) 187–194.

[22] M. Makkee, A.P.G. Kieboom, H. van Bekkhum, Studies on borate esters III. Borate esters of D-mannitol, D-glucitol, D-fructose and D-glucose in water, Reel. Trav. Chim. Pays-Bas 104 (1985) 230–235.

[23] M. Villaverde, N. Bertero, T. Garetto, A. Marchi, Selective liquid-phase hydrogenation of furfural to furfuryl alcohol over Cu-based catalysts, Catal. Today 213 (2013) 87–92.

[24] A. Marchi, D. Gordo, A. Trasarti, C. Apesteguía, Liquid phase hydrogenation of cinnamaldehyde on Cu-based catalysts, Appl. Catal. A Gen 249 (2003) 53–67.

[25] J.I. Di Cosimo, V.K. Diez, M. Xu, E. Iglesia, C.R. Apesteguía, Structure and surface and catalytic properties of Mg-Al basic oxides, J. Catal. 178 (1998) 499–510.

[26] S. Abello, S. Dhir, G. Colet, J. Pérez-Ramírez, Accelerated study of the citral-acetone condensation kinetics over activated Mg-Al hydrotalcite, Appl. Catal. A Gen 325 (2007) 121–129.

[27] A. Dandekar, M.A. Vannice, Determination of the dispersion and surface oxidation states of supported copper catalysts, J. Catal. 178 (1998) 621–639.

[28] S. Yu, E. Kim, S. Park, I.K. Song, J.C. Jung, Isomerization of glucose into fructose over Mg–Al hydrotalcite catalysts, Catal. Commun. 29 (2012) 63–67.

[29] C. Moreau, R. Durand, A. Roux, D. Tichit, Isomerization of glucose into fructose in the presence of cation-exchanged zeolites and hydrotalcites, Appl. Catal. A Gen 193 (2000) 257–264.